

# Current Biology

## CCM-3 Promotes *C. elegans* Germline Development by Regulating Vesicle Trafficking Cytokinesis and Polarity

### Highlights

- CCM-3 promotes for RAB-11-mediated endocytic recycling
- CCM-3 maintains proper localization of Anillin and non-muscle myosin II
- *ccm-3(-/-)* mutants show defective cytokinesis
- CCM-3, along with GCK-1 and CASH-1, effects localization of polarity proteins

### Authors

Swati Pal, Benjamin Lant, Bin Yu, ..., Michael F. Moran, Anne-Claude Gingras, W. Brent Derry

### Correspondence

brent.derry@sickkids.ca

### In Brief

Pal et al. report a key role of the CCM-3/GCK-1/CASH-1 complex in gonadal lumen formation and embryogenesis by mediating endosomal recycling and proper localization of polarity proteins. Conservation of the complex from nematodes to humans might help understand the underlying mechanism of cerebral cavernous malformation (CCM) disease.

# CCM-3 Promotes *C. elegans* Germline Development by Regulating Vesicle Trafficking Cytokinesis and Polarity

Swati Pal,<sup>1</sup> Benjamin Lant,<sup>1</sup> Bin Yu,<sup>1</sup> Ruilin Tian,<sup>1,5</sup> Jiefei Tong,<sup>2</sup> Jonathan R. Krieger,<sup>2</sup> Michael F. Moran,<sup>2,3</sup> Anne-Claude Gingras,<sup>3,4</sup> and W. Brent Derry<sup>1,3,6,\*</sup>

<sup>1</sup>Developmental and Stem Cell Biology Program, Peter Gilgan Centre for Research and Learning, The Hospital for Sick Children, 686 Bay Street, Toronto, ON M5G 0A4, Canada

<sup>2</sup>Cell Biology Program, Peter Gilgan Centre for Research and Learning, The Hospital for Sick Children, 686 Bay Street, Toronto, ON M5G 0A4, Canada

<sup>3</sup>Department of Molecular Genetics, University of Toronto, Toronto, ON M5S 1A8, Canada

<sup>4</sup>Lunenfeld-Tanenbaum Research Institute at Mount Sinai Hospital, 600 University Avenue, Toronto, ON M5G 1X5, Canada

<sup>5</sup>Present address: Integrative Program in Quantitative Biology, University of California, San Francisco, San Francisco, CA 94158, USA

<sup>6</sup>Lead contact

\*Correspondence: [brent.derry@sickkids.ca](mailto:brent.derry@sickkids.ca)

<http://dx.doi.org/10.1016/j.cub.2017.02.028>

## SUMMARY

Cerebral cavernous malformations (CCMs) are vascular defects of the CNS that arise from loss of integrity of the endothelial cells lining blood capillaries, causing leakage of blood into the brain [1]. This results in headaches, seizures, and/or hemorrhagic stroke, depending on the location of the lesion. CCM affects 0.5% of the population and follows an autosomal dominant inheritance pattern caused by mutations in one of the three genes: *CCM1* (gene name *KRIT1*), *CCM2* (also known as malcavernin or *OSM*), and *CCM3* (gene name *PDCD10*) [2, 3], with the earliest onset and most severe prognosis occurring in *CCM3* patients [4]. The three *CCM* genes encode structurally distinct scaffold proteins that function in multiple complexes [5–9]. Using the *C. elegans* germline as a model of multicellular tube development, we show here that CCM-3 is enriched at the luminal membrane of the germline and the contractile ring of dividing cells in the embryo. Loss of *ccm-3* results in defective RAB-11-mediated endocytic recycling, which in turn is necessary for gonadal lumen (rachis) formation, completion of cytokinesis, and localization of cell-surface receptors. CCM-3-mediated localization of anillin and non-muscle myosin to the lateral surfaces of germ cells is required for proper cytoskeletal organization, subsequent oocyte growth, and localization of polarity proteins. Biochemical analysis reveals conservation of the STRIPAK complex and distinct roles for GCK-1 (germinal center kinase III family protein) and striatin/CASH-1 in controlling the localization and function of CCM-3. Taken together, our data establish CCM-3 as a novel regulator of rachis lumenization and polarity establishment during embryogenesis.

## RESULTS AND DISCUSSION

### *ccm-3* Mutants Are Sterile and Contain Multinucleate Germ Cells

We recently developed a *C. elegans* model to investigate the in vivo functions of cerebral cavernous malformation 3 (CCM3) and showed that the worm protein (CCM-3) localizes along the apical (luminal) membrane of both unicellular tubes (excretory canals) and multicellular tubes, including the germline [10]. The nematode germline forms a multicellular tube consisting of two symmetrical U-shaped gonad arms connected by a common uterus in the middle of the body. At the distal end of the gonad, germ cells undergo mitotic proliferation in response to LAG-2 Notch ligand expressed on the distal tip cell (DTC). After they escape the influence of LAG-2/Notch, germ cells mature through the stages of meiotic prophase I until they become fully cellularized oocytes at the proximal end of the gonad (Figure 1A) [11]. During development, germ cells undergo incomplete cytokinesis that generates openings connecting them to the common cytoplasmic core called the rachis (Movie S1). Using the previously characterized deletion allele *tm2806* [10], we observed that homozygous *ccm-3(tm2806)* mutants produce small, round oocytes that render them sterile (Figure 1B). Co-expression of a GFP::CCM-3 translational reporter with the PLC1 $\delta$ 1 membrane marker (mCh::PH) showed localization of CCM-3 to the stable intercellular bridges lining the rachis, the cytoplasm, and to oocyte membranes (Figures 1C and C'). Introduction of the *ccm-3(tm2806)* allele (henceforth designated as *ccm-3(-/-)*) into a strain expressing membrane (GFP::PH) and nuclear (mCh::Histone) markers revealed that the contractile rings connecting germ cells to the lumen lacked defined openings to the rachis (Figures 1D and 1E). To determine when these defects arise, we monitored germline development from the second larval stage (L2) to adulthood and found that the rachis lumen failed to form in *ccm-3(-/-)* mutants at all stages and that the organized arrangement of germ cells became disrupted as the worms reached adulthood (Figures 1D and 1F). Many germ cells were also multinucleated (Figures 1F and 1G), suggesting a role for CCM-3 in cytokinesis. Consistent with this,

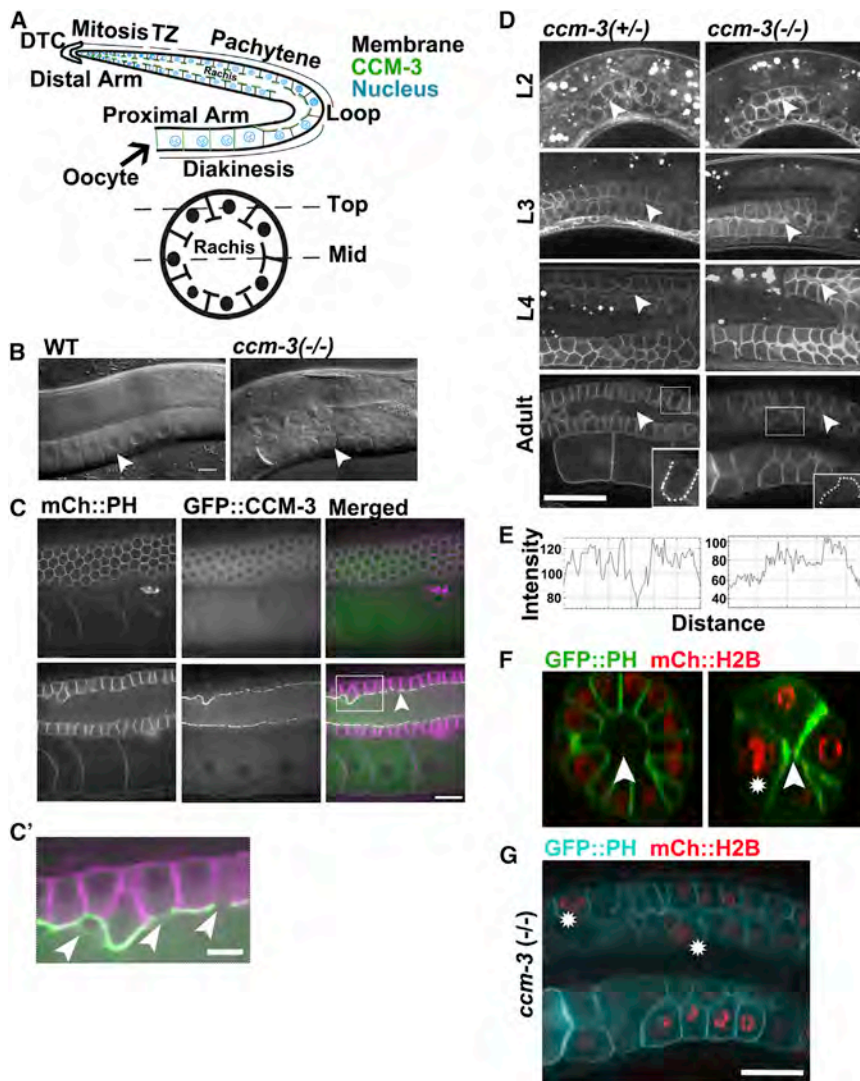


**Figure 1. Loss of *ccm-3* Results in Sterility**

(A) Top: schematic diagram of the mid-focal view of adult *C. elegans* hermaphrodite germline. CCM-3 is depicted in green and localizes to the rachis membrane. As the oocytes become cellularized, CCM-3 is distributed to their membranes. TZ, transition zone. Bottom: diagram of the rachis cross-section, marking the top focal plane and the mid-focal plane.

(B) Differential interference contrast (DIC) images of a wild-type (WT) germline with fully grown, rectangular, oocytes (left; arrowhead) and *ccm-3(-/-)* mutants that contain underdeveloped, round oocytes (right; arrowhead). The mutants are 100% sterile.  $n > 100$ . Scale bar, 25  $\mu\text{m}$ .

(C) Confocal images of a germline expressing GFP::CCM-3 (green) and the membrane marker mCherry::PH (purple). CCM-3 is present in the cytoplasm and colocalizes with mCherry::PH at the membrane lining the rachis (arrowhead). Top: top-focal view, showing the honeycomb pattern arrangement of germ cells in the gonad. Bottom: mid-focal view, revealing the rachis membrane. Scale bar, 15  $\mu\text{m}$ .

(C') Magnified view showing localization of CCM-3 at the rachis bridge from the region delineated by the white rectangle at lower-right panel of (C). Arrowheads point to the bridges connecting germ cells to the rachis. Scale bar, 5  $\mu\text{m}$ .

(D) Mid-focal plane of germlines from the second larval stage (L2) through the adult stage. Left: confocal images of the rachis lumen in *ccm-3(+/-)* worms (arrowheads). Right: confocal images of *ccm-3(-/-)* mutants with a collapsed rachis lumen (arrowheads). Regions delineated with white rectangles in the adult germline are shown in the insets.

(E) Fluorescence intensity was determined along the dotted line marking the germ cell membrane shown in the inset of the adult germlines from (D). The drop in intensity measured for the *ccm-3(+/-)* germ cell corresponds to the gap created by an open contractile ring

connecting to the rachis. Germ cells in *ccm-3(-/-)* worms lacking openings show no decrease in fluorescence intensity.

(F) Cross-sectional view of the germline showing a collapsed rachis (arrowhead) in *ccm-3(-/-)* mutants compared to a *ccm-3(+/-)* germline (left panel). The asterisk marks a multinucleated cell.

(G) Adult *ccm-3(-/-)* mutant germline showing multinucleated germ cells (asterisks).

See also [Movie S1](#).

we observed a 50% reduction in mitotically proliferating *ccm-3(-/-)* germ cells (Figure S1A); from  $\sim 20$  cell diameters in wild-type (WT) [12] and *ccm-3(+/-)* to  $\sim 15$  cell diameters in *ccm-3(-/-)* mutants (Figure 2A, left panels).

### CCM-3 Regulates Endocytic Recycling of Cell Surface Receptors

Since mitotic germ cells are maintained in a proliferative state by binding of the cell-surface Notch receptor GLP-1 to the LAG-2/Notch ligand on the DTC [13], we wondered whether *ccm-3(-/-)* mutants had defective Notch signaling. Immunostaining with anti-GLP-1 antibodies revealed markedly reduced GLP-1 in the mitotic zone of *ccm-3(-/-)* mutants (Figure 2A, right panels). Since Notch receptors are trafficked from the ER to the cell surface and CCM-3 is known to promote endocytic

recycling [10], we hypothesize that recycling of GLP-1 is dependent on CCM-3.

We also observed that pachytene-stage nuclei were present beyond the gonad loop region in *ccm-3(-/-)* mutants, which is normally occupied by growing oocytes in WT animals (Figure 2B, top panels). We wondered whether this was due to defective LET-60/Ras signaling, which is required for pachytene exit as well as maintenance of the rachis [14]. Therefore, we checked phosphorylated MPK-1/ERK (p-MPK-1), a downstream target of Ras signaling, and observed dramatically decreased signal in *ccm-3(-/-)* germlines (Figure 2B, bottom panels). These results suggest a general requirement for CCM-3 in receptor recycling, which is supported by reduced RME-2 receptor on the surface of *ccm-3(-/-)* oocytes. RME-2 mediates endocytosis of yolk proteins such as vitellogenin (VIT-2) that are secreted

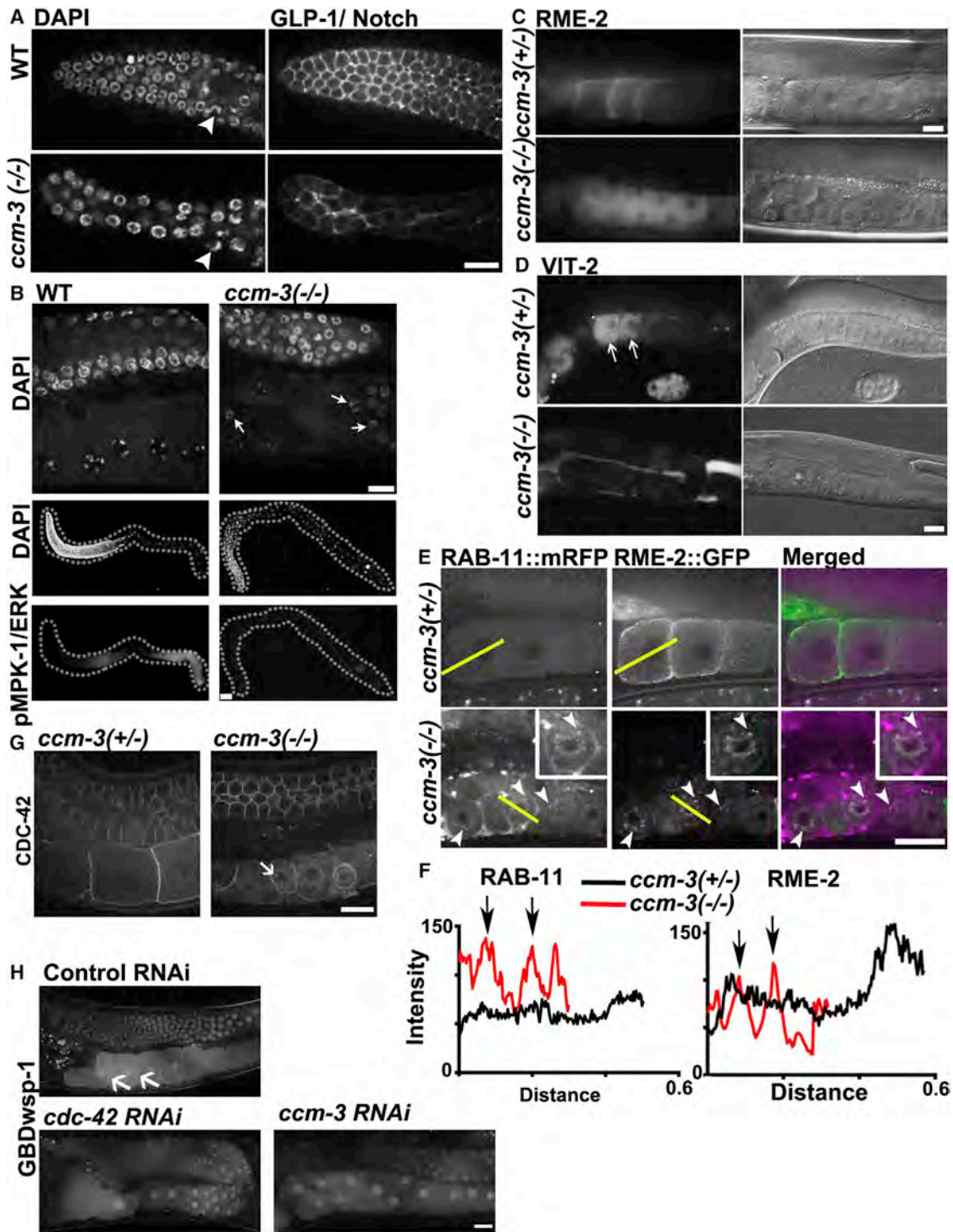


**Figure 2. CCM-3 Is Required for Localization of Cell Surface Receptors**

(A) Gonads dissected from the adult hermaphrodites stained with DAPI and GLP-1 antibodies. The top panels show the mitotic region from wild-type (WT) worms, whereas the bottom panels show the same region of *ccm-3(-/-)* mutants. There are fewer germ cells in the mitotic region of *ccm-3(-/-)* worms compared with WT (see Figure S1A for quantification). Arrowheads point to nuclei with crescent shaped chromatin, indicating meiotic entry. Panels on right show diminished expression of GLP-1 on *ccm-3(-/-)* mitotic germ cells compared with WT. Quantification of mean intensity per unit area reveals ~40% reduction of signal in the mutants ( $p = 0.0005$ ;  $n = 13$  WT and  $n = 29$  *ccm-3(-/-)* worms). Scale bar, 9  $\mu\text{m}$ .

(B) Gonads dissected from adult hermaphrodites were stained with DAPI and anti-diphospho-ERK, which cross-reacts with phosphorylated MPK-1. The top panel shows defective pachytene exit in *ccm-3(-/-)* germlines (arrows point to nuclei at pachytene stage beyond the loop). Scale bars, 11  $\mu\text{m}$ . The lowest panel reveals diminished pMPK-1 staining in *ccm-3(-/-)* mutants. Scale bar, 23  $\mu\text{m}$ .

(legend continued on next page)

into the body cavity from the intestine [15]. In *ccm-3(-/-)* oocytes, RME-2 accumulated in the cytoplasm, concentrating in the perinuclear space (Figures 2C, 2E, and 2F), resulting in accumulation of VIT-2 in the body cavity (Figure 2D). Both GLP-1 and RME-2 undergo regulated internalization, which can then be either degraded in the lysosome or recycled back to the cell surface [15, 16]. Consistent with our previous work showing that CCM-3 promotes endocytic recycling [10], we found that the small GTPase RAB-11, an essential component of endocytic recycling [17], co-localized to the perinuclear region of *ccm-3(-/-)* oocytes with RME-2 (Figures 2E and 2F). This suggests that CCM-3 plays a central role in receptor localization to membranes via RAB-11-mediated recycling.

Defective recycling could contribute to the lack of rachis expansion in *ccm-3(-/-)* mutants since recycling endosomes also play an important role in lumenization of biological tubes [18, 19]. Active Cdc42 associates with RAB11A-positive vesicles during de novo lumenogenesis in MDCK cells [20], and ablation of the *C. elegans* Cdc42 homolog (*cdc-42*) prevents oocytes from taking up yolk protein due to impaired endocytosis [21]. As we saw with RAB-11, CDC-42 mislocalized to puncta in the perinuclear region of *ccm-3(-/-)* oocytes (Figure 2G). Using the translational reporter, mGFP-tagged G protein binding domain of WSP-1 (GBD<sub>WSP-1</sub>), which binds to active GTP-loaded CDC-42, we verified that CDC-42 activity was repressed in *ccm-3(-/-)* mutant oocyte membrane (Figure 2H). Although our data suggest a possible direct role for CCM-3 in RAB-11-dependent recycling, it is also possible that CCM-3 is required for localizing CDC-42 to oocyte membranes. In either case, this would result in defective yolk protein uptake.

### **ccm-3 Mutants Fail in Cytokinesis**

Studies using the *C. elegans* embryo showed that RAB-11 is required for addition of new membrane to the ingressing cleavage furrow [22]. Localization of CCM-3 to intercellular bridges lining the rachis, as well as its effect on RAB-11, prompted us to investigate a potential role in cytokinesis. Examination of early embryonic cell divisions by time-lapse video microscopy revealed that CCM-3 localizes to the cleavage furrow of the one-cell embryo, concentrating at the contractile ring. After completion of cytokinesis, CCM-3 persists as foci on nascent partitions, similar to the midbody remnant (Figure S1B; Movie S2). To determine whether CCM-3 is required for cytokinesis, we imaged early divisions in embryos depleted of CCM-3 using an anillin reporter (GFP::ANI-1). Anillin is an actomyosin scaffold

protein that also localizes to the cleavage furrow during cell division. In embryos depleted of CCM-3, the cleavage furrow formed and cytokinesis apparently completed, but the nascent partition rapidly regressed, generating multinucleate cells (Figure S1C; Movie S3). Given the importance of endocytic recycling for completing cytokinesis [22, 23], we conclude that CCM-3 plays a key role in the recycling of material required for germline development and late stages of cytokinesis. This most likely accounts for the multinucleated germ cells in *ccm-3(-/-)* gonads (Figure 1G). However, given the role of vesicle trafficking in the formation of the worm egg shell, we cannot rule out that cytokinesis defects are the result of osmotic dysregulation.

### **Recruitment of Anillin and Non-muscle Myosin Requires CCM-3**

Since anillin acts as a scaffold for proteins that orchestrate cytokinesis and anillin mutants have similar germline defects as *ccm-3(-/-)* mutants [24, 25], we wondered whether CCM-3 might affect these proteins. Of the three *C. elegans* anillin homologs, ANI-1 and ANI-2 are crucial for development of the germline [25]. The canonical anillin ANI-1 is present on both the rachis and lateral surfaces of germ cells and binds non-muscle myosin II (NMY-2), F-actin, and septin [26–28]. ANI-2 is a shorter anillin isoform that lacks actin and myosin binding domains and localizes exclusively to the rachis bridges, where it antagonizes ANI-1 to prevent completion of cytokinesis [25]. This establishes connections with the rachis core to generate the syncytial gonad. In the absence of ANI-2, the rachis collapses to form multinucleate cells and small round oocytes [24] that resemble *ccm-3* mutants. Since they both localize at the rachis bridges, we next asked whether ANI-2 distribution was affected by CCM-3. In L4-stage *ccm-3(-/-)* mutants, ANI-2 localization on the rachis membrane was unaffected, but by the adult stage, with no expansion of the luminal core, ANI-2 was only found on remnants of rachis membrane and the perinuclear space of underdeveloped oocytes (Figure 3A). Similarly, CCM-3 only persisted on the remains of the rachis membrane after ablation of *ani-2* (Figure S2A). The presence of CCM-3 at the cleavage furrow of the early embryo, where very little ANI-2 has been reported [25, 29], reinforces our conclusion that CCM-3 localization is not dependent on ANI-2. Therefore, ANI-2 prevents contractile ring closure whereas CCM-3 stabilizes the contractile ring, most likely through endocytic recycling.

- (C) Fluorescence and corresponding DIC images of oocytes expressing RME-2::GFP in *ccm-3(+/-)* (top) and *ccm-3(-/-)* mutants (bottom). Scale bar, 25  $\mu$ m.
- (D) Fluorescence and corresponding DIC images of the *ccm-3(+/-)* worms showing uptake of VIT-2::GFP in mature oocytes (top). In *ccm-3(-/-)* mutants, VIT-2::GFP accumulates in the body cavity (bottom). Scale bar, 25  $\mu$ m.
- (E) Confocal images showing localization of RAB-11 and RME-2 in the adult germline. Arrowheads (and inset images) indicate co-localization of these proteins in the perinuclear region of *ccm-3(-/-)* oocytes. There is no significant difference between the mean intensity per unit area for RAB-11 in *ccm-3(-/-)* oocytes ( $p > 0.1$ ;  $n = 30$ ) and *ccm-3(+/-)* oocytes ( $n = 25$ ). Similarly, no statistically significant difference was observed between the mean intensity per unit area for RME-2 in *ccm-3(-/-)* oocytes ( $p > 0.5$ ;  $n = 30$ ) and *ccm-3(+/-)* oocytes ( $n = 25$ ). Scale bar, 22  $\mu$ m.
- (F) Fluorescence quantification of RAB-11 and RME-2 in *ccm-3(+/-)* and *ccm-3(-/-)* worms along the lines across oocytes in (E). The peaks indicated by arrows show increased signal in the perinuclear region of mutant oocytes.
- (G) Confocal images showing altered localization of CDC-42 in the *ccm-3(-/-)* adult germline. The arrow indicates punctate perinuclear accumulation of CDC-42 in the mutant oocyte. Scale bar, 15  $\mu$ m.
- (H) Confocal images showing altered localization of mGFP::GBD<sub>WSP-1</sub> in the *ccm-3(-/-)* adult germline. The top panel shows a germline on control RNAi, where the arrows indicate mGFP::GBD<sub>WSP-1</sub> on the oocyte membrane. This localization is lost when *ccm-3* is knocked down (lower-right panel), similar to depletion of *cdc-42* (lower-left panel). Scale bar, 15  $\mu$ m.

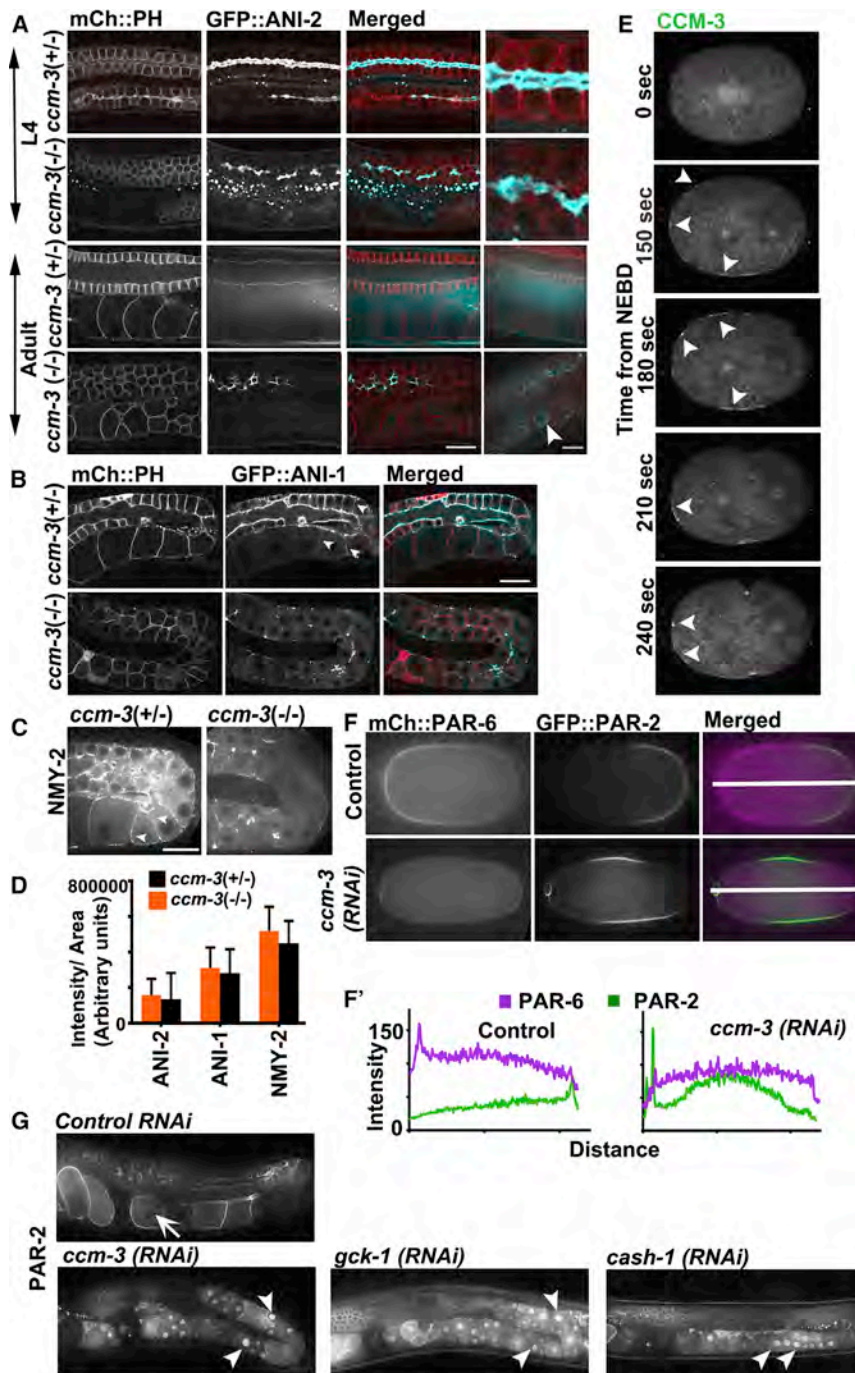


### Figure 3. CCM-3 Is Required for Localization of Anillins, Non-muscle Myosin and Polarity Proteins

(A) Confocal images showing the distribution of GFP::ANI-2 (blue) and the membrane marker, mCherry::PH (red) in the germlines of fourth larval stage (L4) and adult hermaphrodites. Although ANI-2 is localized to the rachis membrane in both *ccm-3(+/-)* and *ccm-3(-/-)* mutants at the L4 stage (first and second panels from the top), it is found only at remnants of the rachis membrane and in the perinuclear region (arrowhead) of adult germlines (third and fourth panels from the top). The rightmost panels are magnifications of images showing merged fluorescence. Quantification of mean intensity per unit area reveals no significant difference in ANI-2 signal in *ccm-3(-/-)* germlines ( $p > 0.6$ ;  $n = 16$  *ccm-3(+/-)* and  $n = 15$  *ccm-3(-/-)* worms). Scale bar, 15  $\mu\text{m}$ . See also [Figures S2A](#) and [S2B](#).

(B) Confocal images showing loss of GFP::ANI-1 from the cortical surface of germ cells in *ccm-3(-/-)* mutants. Arrowheads indicate localization of ANI-1 on the cortical surface of *ccm-3(+/-)* worms. Quantification of mean intensity per unit area reveals no significant difference between total ANI-1 level in the *ccm-3(+/-)* and *ccm-3(-/-)* germlines, ( $p = 0.3$ ;  $n = 32$  *ccm-3(+/-)* and  $n = 42$  *ccm-3(-/-)* worms). Quantification of ANI-1 and membrane marker at the lateral surface of the growing oocytes revealed a 47% reduction in ANI-1 ( $p = 0.002$ ;  $n = 28$  *ccm-3(+/-)* and  $n = 28$  *ccm-3(-/-)* oocytes). Scale bar, 22  $\mu\text{m}$ .

(C) Confocal images show loss of NMY-2::GFP from the cortical surface of germ cells in *ccm-3(-/-)* mutants. Arrowheads indicate localization of NMY-2 on the cortical surface of *ccm-3(+/-)* worms. Quantification of mean intensity per unit area of total NMY-2 signal reveals no significant difference between *ccm-3(-/-)* germlines ( $p > 0.05$ ;  $n = 20$  *ccm-3(+/-)* and  $n = 32$  *ccm-3(-/-)* worms), although there was a 26% decrease in the signal on the lateral surface of the *ccm-3(-/-)* oocytes ( $p = 0.0005$ ;  $n = 27$  *ccm-3(+/-)* and  $n = 40$  *ccm-3(-/-)* oocytes). Scale bar, 17  $\mu\text{m}$ . See also [Figure S2C](#).

(D) Quantification of mean intensity per area for total ANI-2, ANI-1, and NMY-2 in *ccm-3(+/-)* and *ccm-3(-/-)* germlines. Error bars indicate the SEM. (E) Confocal live imaging of an embryo expressing GFP::CCM-3 showing migration of CCM-3 to the anterior of the embryo (arrowhead). The anterior side is on the left. Time 0 corresponds to the point of nuclear envelope breakdown (NEBD). Scale bar, 15  $\mu\text{m}$ .

(F) Confocal images of embryos co-expressing mCherry::PAR-6 (magenta) and GFP::PAR-2 (green) on control (top) and *ccm-3(RNAi)* (bottom). Both polarity proteins are mislocalized in embryos depleted of CCM-3.

(F') Intensity (a.u.) of PAR-2 and PAR-6 proteins along the line across embryos (left) in (E).

(G) GFP::PAR-2 mislocalizes to meiotic nuclei (arrowheads) after ablation of *ccm-3*, *gck-1* or *cash-1* by RNAi. Arrow indicates exclusion of PAR-2 from the nucleus on control RNAi. Arrowheads indicate excluded PAR-2. Quantification of mean intensity per unit area (a.u.) reveals 1.6-fold increase in PAR-2 signal on *ccm-3(RNAi)* ( $n = 14$ ) compared with control RNAi ( $n = 13$ ;  $p = 0.016$ ). Scale bar, 22  $\mu\text{m}$ .

See also [Figures S1B](#) and [S1C](#) and [Movies S2](#), [S3](#), and [S4](#).

Beyond the well-documented role of anillin in cytokinesis, it has also been implicated in enforcing junctional integrity of epithelial cells through Rho-GTP accumulation and actomyosin

organization [30]. Worms lack junctions in the germline, but ANI-1 is present on the rachis and lateral membranes of developing germ cells [25]. Although localization of ANI-1 at

the cleavage furrow (both the germline rachis and the embryo) was unaffected, localization at the lateral surfaces of germ cells was greatly diminished in *ccm-3(-/-)* mutants (Figure 3B). Anillins are required for proper localization of NMY-2, which is required for actomyosin organization [25, 30]. In *C. elegans*, cortical NMY-2 and its regulatory light chain MLC-4 regulate cytoplasmic streaming, cellularization, and membrane maintenance necessary for oocyte growth [31–33]. NMY-2 was also lost from the lateral surfaces of the germ cells in *ccm-3(-/-)* mutants (Figure 3C), similar to ablation of *ani-1*, but its localization at the membrane lining the dilated rachis was unperturbed (Figure S2C). We conclude that CCM-3 is required for organizing anillin and myosin on the cortical surfaces of germ cells to promote oocyte growth.

### CCM-3 Regulates Polarity

Fertilization establishes polarity of the *C. elegans* embryo, in part through the activity of non-muscle myosin [34]. The abnormal NMY-2 distribution in *ccm-3(-/-)* germlines (Figure 3C) prompted us to investigate whether CCM-3 affects contractile events and polarity. Immediately after fertilization, actomyosin-mediated cortical constrictions create reciprocal cytoplasmic flow toward the posterior pole to establish anterior-posterior (A/P) polarity, with the PAR-3/PAR-6/PKC-3 (aPAR) complex localizing to the anterior pole and PAR-2/PAR-1 to the posterior pole [35]. In the subsequent maintenance phase, CDC-42 restricts myosin and aPAR proteins to the anterior pole of the embryo [36–38]. We suspected a role for CCM-3 in the regulation of polarity after observing a range of cytokinesis defects in early embryos depleted of *ccm-3* that ranged from lack of actomyosin contractions (7 out of 17 embryos) and pseudocleavage (9 out of 17 embryos) to regression of the cleavage furrow (1 out of 17 embryos) (Movie S4), which is reminiscent of *nmy-2* depletion [34, 39]. To determine whether CCM-3 affects A/P polarity in the embryo, we examined the localization of the polarity proteins PAR-6 and PAR-2, which occupy the anterior and posterior domains, respectively. Ablation of *ccm-3* disrupted the localization of these proteins (Figure 3F). For example, in 10 out of 15 embryos, PAR-2 was distributed in patches on the cortex and often mislocalized to the lateral side (Figures 3F and 3F'; Movie S4), similar to ablation of *nmy-2* or *mlc-4* [34, 39, 40]. In these same embryos, PAR-6 was found to occupy the entire cortex. We also observed two embryos in which PAR-2 was distributed all around the cortex whereas PAR-6 was sequestered in the cytoplasm. Two other embryos had PAR-6 localized to a small patch on the cortex, whereas the rest of the cortex was occupied by PAR-2. Time-lapse imaging revealed localization of GFP::CCM-3 to the anterior cortex at the time of polarity establishment, supporting a role in polarization of the embryo (Figure 3E). CCM-3 also had strong effects on PAR-2 localization in the germline. Although there was only a modest (1.6-fold) increase in PAR-2 after ablation of *ccm-3*, we observed a dramatic re-localization of the protein from germ cell membranes to nuclei in the meiotic region (Figure 3G). Taken together, these results establish CCM-3 as a novel determinant of cell polarity.

### Structure-Function Analysis of CCM-3

Participation of CCM3 in diverse biological processes is not surprising considering its ability to form multiple complexes with a

variety of proteins such as CCM2, paxillin, striatin, and germinal center kinases (GCKs) [6, 7, 9, 41]. In human cells, the majority of CCM3 resides in the STRIPAK complex, where it interacts with GCK III proteins (MST4, STK24, and STK25) through its N-terminal homodimerization domain and striatin via its C-terminal FAT domain [6, 9]. The critical residues mediating these interactions are conserved in *C. elegans* (Figure 4A), and we previously demonstrated a physical interaction between CCM-3 and the worm GCK III ortholog GCK-1 [10]. Like CCM-3, GCK-1 localizes to rachis bridges lining the lumen of the germline and the cleavage furrow of dividing cells in the early embryo (Figure S2D). The germlines of *gck-1(km15)* mutants have a collapsed rachis lumen and underdeveloped oocytes that are indistinguishable from those of *ccm-3(-/-)* mutants. PAR-2 also mislocalizes to meiotic germ cell nuclei upon depletion of *gck-1* (Figure 3G, lower-middle panel), suggesting a common link to polarity establishment through CCM-3/GCK-1. Unexpectedly, ablation of *gck-1* caused GFP::CCM-3 to mislocalize to germ cell nuclei, although a small amount was still present on sections of the collapsed rachis membrane (Figure S2A, middle panel). Conversely, ablation of *ccm-3* displaced GCK-1::GFP from the rachis membrane, where it accumulated in the cytoplasm but not nuclei (Figure S2E). Knockdown of the striatin ortholog *cash-1* by RNAi caused rachis collapse in 20% of worms, small oocytes in 44% of worms, and nuclear mislocalization of PAR-2::GFP in 50% of worms (Figure 3G, lower-right panel). Based on these observations, we predict the existence of a conserved worm STRIPAK complex on the luminal membrane of the germline. But what interactions with CCM-3 are important for rachis formation and embryonic development?

To define the functional significance of interactions between CCM-3, GCK-1, and CASH-1, we created GFP-tagged constructs in which the conserved residues of CCM-3 required for binding GCK-1 or CASH-1 were mutated and then expressed in *ccm-3(-/-)* mutants [9, 42, 43]. Mutations in the N-terminal domain required for binding GCK-1 (L41D, A44D, L63D, and L64D) caused GFP::CCM-3 to localize to germ cell nuclei similar to WT CCM-3 in worms treated with *gck-1(RNAi)* (Figures 4B and S2A). The N-terminal mutant failed to rescue germ cell morphology and sterility of *ccm-3(-/-)*, reinforcing the importance of the interaction between CCM-3 and GCK-1 and in agreement with Rehai-Bell et al. [44]. The C terminus of CCM3 binds striatin/CASH-1, paxillin, and CCM2 [9, 41], and mutation of the four lysine residues (K132A, K139A, K172A, and K179A) crucial for binding striatin/CASH-1 caused displacement of GFP::CCM-3 from the rachis membrane to the cytoplasm, but not mislocalization to nuclei (Figure 4B). Although there was no improvement in rachis morphology, about 60% of *ccm-3(-/-)* worms expressing the C-terminal CCM-3 mutant were fertile and produced embryos, some of which developed to the comma stage (~330 min post-fertilization) prior to arresting. Thus, the interaction with GCK-1 is crucial for all functions of CCM-3, but its interaction with CASH-1 is dispensable until later stages of embryonic development. We propose that binding of CCM-3 to GCK-1 keeps CCM-3 in the cytoplasm and supports proper oocyte development and that binding to CASH-1 localizes CCM-3/GCK-1 to the membrane (Figure 4E). Mammalian CCM3 mediates interactions between the GCK III kinases and

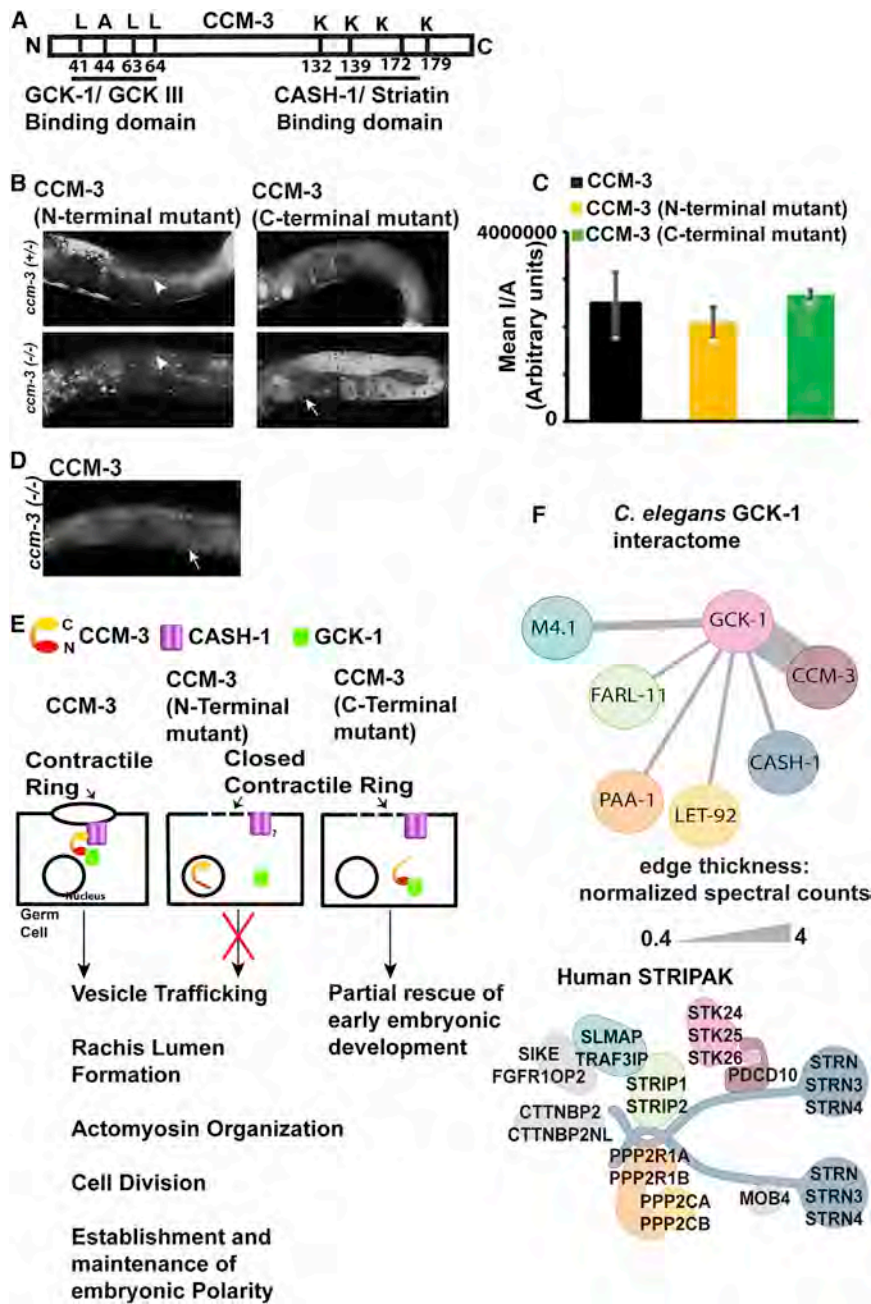


**Figure 4. CCM-3 Interaction with GCK-1 and CASH-1 Is Required for Its Proper Localization and Function**

(A) Schematic representation of CCM-3 protein depicting the conserved N-terminal and C-terminal residues required for binding with GCK-1 and CASH-1, respectively.

(B) Confocal images of germlines from *ccm-3*(+/-) (top) and *ccm-3*(-/-) (bottom) hermaphrodites expressing GFP-tagged mutant CCM-3 proteins. The N-terminal CCM-3 mutant (L41A, A44D, L63, and L64D) is unable to bind GCK-1 and mislocalizes to meiotic nuclei (right; indicated by arrowhead). The C-terminal CCM-3 mutant (K132A, K139A, K172A, and K179A) does not bind CASH-1, preventing its localization to the rachis membrane (left). In *ccm-3*(-/-) mutants (bottom), expression of neither of the mutant proteins could rescue rachis lumen defects, but early embryonic development (indicated by arrow) was restored by expression of the C-terminal mutant. See also Figures S2A and S2E.

(C) Quantification of GFP-tagged CCM-3 mutant proteins. Error bars indicate the SEM.

(D) Rescue of sterility in *ccm-3*(-/-) mutants by expression of WT CCM-3 tagged with GFP. The arrow indicates a developing embryo.

(E) Model depicting how interactions of CCM-3 with GCK-1 and CASH-1/striatin affect germline and embryonic development.

(F) GCK-1-interacting proteins identified by immunoprecipitation followed by mass spectrometry. The interactome map in *C. elegans* (top) reveals conservation of the STRIPAK components compared with those of humans (bottom). Line thickness is proportional to normalized spectral counts (total number of peptides divided by protein length) for the prey. The orthologous proteins in the two species are color coded. See also Table S1.

the other STRIPAK proteins [9]. To determine whether these physical interactions are conserved, we immunoprecipitated GCK-1::GFP from whole-worm lysate and identified the associated proteins by mass spectrometry. Several STRIPAK components were recovered as major interactors (Figure 4F; Table S1), but the absence of KRI-1/CCM1 in the recovered peptides reinforces the view that CCM3 functions by a mechanism distinct from that of CCM1/2 [10, 45].

In conclusion, we used a combination of genetics, cell biology, and proteomics to demonstrate that CCM-3 functions as a key node that integrates multiple signaling pathways to promote germline tube development through diverse yet interlinked processes, including endocytic recycling, actomyosin organization,

cytokinesis, and cell polarity. This work has important implications for understanding the aggressive nature of CCM disease in patients with mutations in the *CCM3* gene.

#### SUPPLEMENTAL INFORMATION

Supplemental Information includes Supplemental Experimental Procedures, two figures, one table, and four movies and can be found with this article online at <http://dx.doi.org/10.1016/j.cub.2017.02.028>.

#### AUTHOR CONTRIBUTIONS

S.P. performed most of the experiments. B.L., B.Y., R.T., and W.B.D. performed experiments. J.T., J.R.K., and M.F.M. performed mass spectrometry

experiments. A.-C.G. provided input on mass spectrometry and design of structure-function experiments. S.P. and W.B.D. wrote the manuscript.

## ACKNOWLEDGMENTS

W.B.D. and A.-C.G. were supported by the Canadian Institutes for Health Research (MOP-123433). W.B.D. also received support from Angioma Alliance Canada. A.-C.G. is a Canada Research Chair in Functional Proteomics and the Lea Reichmann Chair in Cancer Proteomics. M.F.M. is a Canada Research Chair in Molecular Signatures. B.L. was supported by a Restracom fellowship from the Hospital for Sick Children Research Institute. Strains were provided by the *Caenorhabditis* Genetics Center (funded by the NIH Office of Research Infrastructure Programs, P40 OD010440). ANI-1::GFP, ANI-2::GFP, and NMY-2::GFP strains were provided by Dr. Jean-Claude Labbe. Anti-GLP-1 antibody was provided by Dr. Judith Kimble. The strain expressing mRFP::RAB-11 under germline specific promoter was a kind gift from Dr. Barth D. Grant. We are grateful to Dr. Salim Seyfried, Dr. Ian Scott, and Abigail Mateo for insightful comments.

Received: September 14, 2016

Revised: February 1, 2017

Accepted: February 13, 2017

Published: March 9, 2017

## REFERENCES

- Fischer, A., Zalvide, J., Faurobert, E., Albiges-Rizo, C., and Tournier-Lasserre, E. (2013). Cerebral cavernous malformations: from CCM genes to endothelial cell homeostasis. *Trends Mol. Med.* **19**, 302–308.
- Laberge-le Couteux, S., Jung, H.H., Labauge, P., Houtteville, J.P., Lescoat, C., Cecillon, M., Marechal, E., Joutel, A., Bach, J.F., and Tournier-Lasserre, E. (1999). Truncating mutations in CCM1, encoding KRIT1, cause hereditary cavernous angiomas. *Nat. Genet.* **23**, 189–193.
- Craig, H.D., Günel, M., Cepeda, O., Johnson, E.W., Ptacek, L., Steinberg, G.K., Ogilvy, C.S., Berg, M.J., Crawford, S.C., Scott, R.M., et al. (1998). Multilocus linkage identifies two new loci for a mendelian form of stroke, cerebral cavernous malformation, at 7p15-13 and 3q25.2-27. *Hum. Mol. Genet.* **7**, 1851–1858.
- Shenkar, R., Shi, C., Rebeiz, T., Stockton, R.A., McDonald, D.A., Mikati, A.G., Zhang, L., Austin, C., Akers, A.L., Gallione, C.J., et al. (2015). Exceptional aggressiveness of cerebral cavernous malformation disease associated with PDCD10 mutations. *Genet. Med.* **17**, 188–196.
- Zawistowski, J.S., Stalheim, L., Uhlik, M.T., Abell, A.N., Ancrile, B.B., Johnson, G.L., and Marchuk, D.A. (2005). CCM1 and CCM2 protein interactions in cell signaling: implications for cerebral cavernous malformations pathogenesis. *Hum. Mol. Genet.* **14**, 2521–2531.
- Goudreaux, M., D'Ambrosio, L.M., Kean, M.J., Mullin, M.J., Larsen, B.G., Sanchez, A., Chaudhry, S., Chen, G.I., Sicheri, F., Nesvizhskii, A.I., et al. (2009). A PP2A phosphatase high density interaction network identifies a novel striatin-interacting phosphatase and kinase complex linked to the cerebral cavernous malformation 3 (CCM3) protein. *Mol. Cell. Proteomics* **8**, 157–171.
- Hilder, T.L., Malone, M.H., Bencharit, S., Colicelli, J., Haystead, T.A., Johnson, G.L., and Wu, C.C. (2007). Proteomic identification of the cerebral cavernous malformation signaling complex. *J. Proteome Res.* **6**, 4343–4355.
- Lampugnani, M.G., Orsenigo, F., Rudini, N., Maddaluno, L., Boulday, G., Chapon, F., and Dejana, E. (2010). CCM1 regulates vascular-lumen organization by inducing endothelial polarity. *J. Cell Sci.* **123**, 1073–1080.
- Kean, M.J., Ceccarelli, D.F., Goudreaux, M., Sanches, M., Tate, S., Larsen, B., Gibson, L.C., Dery, W.B., Scott, I.C., Pelletier, L., et al. (2011). Structure-function analysis of core STRIPAK Proteins: a signaling complex implicated in Golgi polarization. *J. Biol. Chem.* **286**, 25065–25075.
- Lant, B., Yu, B., Goudreaux, M., Holmyard, D., Knight, J.D., Xu, P., Zhao, L., Chin, K., Wallace, E., Zhen, M., et al. (2015). CCM-3/STRIPAK promotes seamless tube extension through endocytic recycling. *Nat. Commun.* **6**, 6449.
- Hirsh, D., Oppenheim, D., and Klass, M. (1976). Development of the reproductive system of *Caenorhabditis elegans*. *Dev. Biol.* **49**, 200–219.
- Crittenden, S.L., Troemel, E.R., Evans, T.C., and Kimble, J. (1994). GLP-1 is localized to the mitotic region of the *C. elegans* germ line. *Development* **120**, 2901–2911.
- Henderson, S.T., Gao, D., Lambie, E.J., and Kimble, J. (1994). *lag-2* may encode a signaling ligand for the GLP-1 and LIN-12 receptors of *C. elegans*. *Development* **120**, 2913–2924.
- Lee, M.H., Ohmachi, M., Arur, S., Nayak, S., Francis, R., Church, D., Lambie, E., and Schedl, T. (2007). Multiple functions and dynamic activation of MPK-1 extracellular signal-regulated kinase signaling in *Caenorhabditis elegans* germline development. *Genetics* **177**, 2039–2062.
- Grant, B., and Hirsh, D. (1999). Receptor-mediated endocytosis in the *Caenorhabditis elegans* oocyte. *Mol. Biol. Cell* **10**, 4311–4326.
- Bray, S.J. (2006). Notch signalling: a simple pathway becomes complex. *Nat. Rev. Mol. Cell Biol.* **7**, 678–689.
- Ullrich, O., Reinsch, S., Urbé, S., Zerial, M., and Parton, R.G. (1996). Rab11 regulates recycling through the pericentriolar recycling endosome. *J. Cell Biol.* **135**, 913–924.
- Desclozeaux, M., Venturato, J., Wylie, F.G., Kay, J.G., Joseph, S.R., Le, H.T., and Stow, J.L. (2008). Active Rab11 and functional recycling endosome are required for E-cadherin trafficking and lumen formation during epithelial morphogenesis. *Am. J. Physiol. Cell Physiol.* **295**, C545–C556.
- Blasky, A.J., Mangan, A., and Prekeris, R. (2015). Polarized protein transport and lumen formation during epithelial tissue morphogenesis. *Annu. Rev. Cell Dev. Biol.* **31**, 575–591.
- Bryant, D.M., Datta, A., Rodríguez-Fraticelli, A.E., Peränen, J., Martín-Belmonte, F., and Mostov, K.E. (2010). A molecular network for de novo generation of the apical surface and lumen. *Nat. Cell Biol.* **12**, 1035–1045.
- Balklava, Z., Pant, S., Fares, H., and Grant, B.D. (2007). Genome-wide analysis identifies a general requirement for polarity proteins in endocytic traffic. *Nat. Cell Biol.* **9**, 1066–1073.
- Skop, A.R., Bergmann, D., Mohler, W.A., and White, J.G. (2001). Completion of cytokinesis in *C. elegans* requires a brefeldin A-sensitive membrane accumulation at the cleavage furrow apex. *Curr. Biol.* **11**, 735–746.
- Albertson, R., Riggs, B., and Sullivan, W. (2005). Membrane traffic: a driving force in cytokinesis. *Trends Cell Biol.* **15**, 92–101.
- Amini, R., Goupil, E., Labella, S., Zetka, M., Maddox, A.S., Labbé, J.C., and Chartier, N.T. (2014). *C. elegans* Anillin proteins regulate intercellular bridge stability and germline syncytial organization. *J. Cell Biol.* **206**, 129–143.
- Maddox, A.S., Habermann, B., Desai, A., and Oegema, K. (2005). Distinct roles for two *C. elegans* anillins in the gonad and early embryo. *Development* **132**, 2837–2848.
- Field, C.M., and Alberts, B.M. (1995). Anillin, a contractile ring protein that cycles from the nucleus to the cell cortex. *J. Cell Biol.* **131**, 165–178.
- Oegema, K., Savoian, M.S., Mitchison, T.J., and Field, C.M. (2000). Functional analysis of a human homologue of the *Drosophila* actin binding protein anillin suggests a role in cytokinesis. *J. Cell Biol.* **150**, 539–552.
- Straight, A.F., Field, C.M., and Mitchison, T.J. (2005). Anillin binds non-muscle myosin II and regulates the contractile ring. *Mol. Biol. Cell* **16**, 193–201.
- Chartier, N.T., Salazar Ospina, D.P., Benkemoun, L., Mayer, M., Grill, S.W., Maddox, A.S., and Labbé, J.C. (2011). PAR-4/LKB1 mobilizes non-muscle myosin through anillin to regulate *C. elegans* embryonic polarization and cytokinesis. *Curr. Biol.* **21**, 259–269.
- Reyes, C.C., Jin, M., Breznau, E.B., Espino, R., Delgado-Gonzalo, R., Goryachev, A.B., and Miller, A.L. (2014). Anillin regulates cell-cell junction integrity by organizing junctional accumulation of Rho-GTP and actomyosin. *Curr. Biol.* **24**, 1263–1270.

31. Wolke, U., Jezuit, E.A., and Priess, J.R. (2007). Actin-dependent cytoplasmic streaming in *C. elegans* oogenesis. *Development* *134*, 2227–2236.
32. Nadarajan, S., Govindan, J.A., McGovern, M., Hubbard, E.J., and Greenstein, D. (2009). MSP and GLP-1/Notch signaling coordinately regulate actomyosin-dependent cytoplasmic streaming and oocyte growth in *C. elegans*. *Development* *136*, 2223–2234.
33. Kachur, T.M., Audhya, A., and Pilgrim, D.B. (2008). UNC-45 is required for NMY-2 contractile function in early embryonic polarity establishment and germline cellularization in *C. elegans*. *Dev. Biol.* *314*, 287–299.
34. Guo, S., and Kemphues, K.J. (1996). A non-muscle myosin required for embryonic polarity in *Caenorhabditis elegans*. *Nature* *382*, 455–458.
35. Munro, E., Nance, J., and Priess, J.R. (2004). Cortical flows powered by asymmetrical contraction transport PAR proteins to establish and maintain anterior-posterior polarity in the early *C. elegans* embryo. *Dev. Cell* *7*, 413–424.
36. Gotta, M., Abraham, M.C., and Ahringer, J. (2001). CDC-42 controls early cell polarity and spindle orientation in *C. elegans*. *Curr. Biol.* *11*, 482–488.
37. Aceto, D., Beers, M., and Kemphues, K.J. (2006). Interaction of PAR-6 with CDC-42 is required for maintenance but not establishment of PAR asymmetry in *C. elegans*. *Dev. Biol.* *299*, 386–397.
38. Schonegg, S., and Hyman, A.A. (2006). CDC-42 and RHO-1 coordinate acto-myosin contractility and PAR protein localization during polarity establishment in *C. elegans* embryos. *Development* *133*, 3507–3516.
39. Cuenca, A.A., Schetter, A., Aceto, D., Kemphues, K., and Seydoux, G. (2003). Polarization of the *C. elegans* zygote proceeds via distinct establishment and maintenance phases. *Development* *130*, 1255–1265.
40. Shelton, C.A., Carter, J.C., Ellis, G.C., and Bowerman, B. (1999). The nonmuscle myosin regulatory light chain gene *mlc-4* is required for cytokinesis, anterior-posterior polarity, and body morphology during *Caenorhabditis elegans* embryogenesis. *J. Cell Biol.* *146*, 439–451.
41. Li, X., Zhang, R., Zhang, H., He, Y., Ji, W., Min, W., and Boggon, T.J. (2010). Crystal structure of CCM3, a cerebral cavernous malformation protein critical for vascular integrity. *J. Biol. Chem.* *285*, 24099–24107.
42. Zhang, M., Dong, L., Shi, Z., Jiao, S., Zhang, Z., Zhang, W., Liu, G., Chen, C., Feng, M., Hao, Q., et al. (2013). Structural mechanism of CCM3 heterodimerization with GCKIII kinases. *Structure* *21*, 680–688.
43. Ceccarelli, D.F., Laister, R.C., Mulligan, V.K., Kean, M.J., Goudreault, M., Scott, I.C., Derry, W.B., Chakrabarty, A., Gingras, A.C., and Sicheri, F. (2011). CCM3/PDCD10 heterodimerizes with germinal center kinase III (GCKIII) proteins using a mechanism analogous to CCM3 homodimerization. *J. Biol. Chem.* *286*, 25056–25064.
44. Rehai-Bell, K., Love, A., Werner, M.E., MacLeod, I., Yates, J.R., 3rd, and Maddox, A.S. (2017). A Sterile 20 family kinase and its co-factor CCM-3 regulate contractile ring proteins on germline intercellular bridges. *Curr. Biol.* Published online March 9, 2017. <http://dx.doi.org/10.1016/j.cub.2017.01.058>.
45. Yoruk, B., Gillers, B.S., Chi, N.C., and Scott, I.C. (2012). Ccm3 functions in a manner distinct from Ccm1 and Ccm2 in a zebrafish model of CCM vascular disease. *Dev. Biol.* *362*, 121–131.